Mechanical Properties of a Particle-Strengthened Polyurethane Foam

S. H. GOODS,[1] C. L. NEUSCHWANGER,[2] L. L. WHINNERY,[1] W. D. NIX[3]

[1] Sandia National Laboratories, Livermore, California 94550

[2] Hewlett-Packard Company, Palo Alto, California 94304

[3] Department of Materials Science and Engineering, Stanford University, Stanford, California 94350

Received 16 March 1999; accepted 15 June 1999

ABSTRACT: Quasi-static compression tests have been performed on polyurethane foam specimens. The modulus of the foam exhibited a power-law dependence with respect to density of the form: $E^* \propto (\rho^*)^n$, where $n = 1.7$. The modulus data are described well by a simple geometric model (based on the work of Gibson and Ashby) for a closed-cell foam in which the stiffness of the foam is governed by the flexure of the cell struts and cell walls. The compressive strength of the foam is also found to follow a power-law behavior with respect to foam density. In this instance, Euler buckling is used to explain the density dependence. The modulus of the foam was modified by addition of gas-atomized, spherical, aluminum powder. Additions of 30 and 50 wt % Al measurably increased the foam modulus, but without a change in the density dependence. However, there was no observable increase in modulus with 5 and 10 wt % additions of the metal powder. Strength was also increased at high loading fractions of powder. The increase in modulus and strength could be predicted by combining the Gibson–Ashby model, referred to above, with a well-known model describing the effect on modulus of a rigid dispersoid in a compliant matrix. © 1999 John Wiley & Sons, Inc. J Appl Polym Sci 74: 2724–2736, 1999

Key words: mechanical properties; foam; particle-strengthening; modulus

INTRODUCTION

Foams are widely used in a variety of applications for the advantages they bring in energy absorption characteristics, thermal properties, and specific strength. A closed-cell foam consists of two phases: a solid phase, from which the structure of the foam is formed, and a gaseous phase, which may be derived from any of several sources, either physical or chemical. Polymeric foams are the most common and, depending on their structure (that is, whether or not the foam is open- or closed-cell), are used in applications involving cushioning, thermal insulation, and structural support.

The application for which a particular polymer foam is suited also depends on the intrinsic properties of the polymer (which determine whether the foam is flexible or rigid). For example, foam derived from a polymer having a glass transition temperature (T_g) near ambient will exhibit greater ductility and rate sensitivity in its mechanical response than a foam derived from a polymer with a high T_g.[1] The properties of foams also depend on the structure and geometry of the cellular structure. A foam comprised of a closed-cell structure will be more thermally insulating

Correspondence to: S. H. Goods.

Contract grant sponsor: U.S. Department of Energy; contract grant number: DE-AC04-94AL85000.

Journal of Applied Polymer Science, Vol. 74, 2724–2736 (1999)

 CCC 0021-8995/99/112724-13

than an open-cell foam. Lastly, foams with cell structures having high aspect ratios will exhibit anisotropic behavior with respect to a variety of mechanical and physical properties.[2,3]

A foam can also be a composite material incorporating other solids into the host polymer in order to modify certain physical (modulus, thermal conductivity, or coefficient of thermal expansion [CTE]) or mechanical (strength, toughness) properties. Examples of such additives or fillers include metal, glass, and ceramic powders. These composite foams can possess even better strength to weight ratios and energy absorption properties than the baseline foams formed solely from the matrix polymer.[4]

The present work examines the effect of increasing loading fractions of an aluminum powder additive on the mechanical properties of a structural polyurethane (PU) foam. The principal consideration for the use of a metallic filler phase, such as aluminum, is the effect that the additive may have on the insulating qualities of the foam. For example, metal powders or fibers can significantly increase the thermal conductivity of foams. This can be advantageous when the foam is used in a storage or shipping container to encapsulate a structure that is self-heating. In such an instance, the ability to tailor the dissipative properties of the foam is important in order to keep the internal temperature of a container acceptably low.

It is this interest in modifying the thermal characteristics of a foam that motivated the current work. If a metal-loaded foam is to be used in such an application, the influence of the filler phase on mechanical properties must also be considered (as the foam must also protect a component from shock or impact). Specifically, the present work examines the effect of increasing loading fractions of a 2-μm aluminum powder additive on the modulus and strength of a polyurethane foam called CRETE. The intrinsic mechanical properties of this foam, without the addition of a filler phase, have been presented in detail elsewhere[5] and, along with additional data, are reviewed here for the sake of completeness.

EXPERIMENTAL

Formulation and Processing of CRETE Foam

The foam chosen for this study is called CRETE. CRETE is formulated without toluene diisocyanate (TDI), which has been identified a potential human carcinogen. Rather, it incorporates a modified diphenylmethane diisocyanate (MMDI).[5] It is a rigid, closed-cell, water-blown polyurethane foam formulated from the following constituents.

1. Voranol 490™, a polyether polyol, made from polypropylene oxide and a sucrose/glycerin base, available from Dow Chemical. The manufacturer specifies the following properties: Density (25°C), 1.1 g/cm^3; typical hydroxyl number, 490 mg KOH equiv/g of resin; functionality, 4.3 (calculated); average molecular weight, 460 g/mol; viscosity (25°C), 5572 centipoise (cps).
2. DC193™, a silicone glycol copolymer surfactant from Air Products with an average hydroxyl number of 75.
3. Polycat 17™, a tertiary amine catalyst (trimethyl-*N*-hydroxyethyl propylene diamine) available from Air Products with an average hydroxyl number of 400.
4. Distilled water, added in various amounts as a chemical blowing agent to produce carbon dioxide. The amount of water added determines the foam density as the water controls the rise within the foam.
5. Isonate 143L™, modified MMDI available from Dow Chemical. The manufacturer specifies the following properties for Isonate 143L: Isocyanate equivalent weight, 144.5 g; content by weight, 29.2%; functionality, 2.1; viscosity (25°C), 33 cps.

Components 1–4 were stirred together by hand. The isocyanate was then added, and the complete mixture is stirred for 1 min using a Conn mixing blade. The addition of the isocyanate initiates the rise of the foam by reacting with the water to form CO_2. The mixture was poured into a waxed cylindrical mold and sealed with a hand-tightened clamp. This tooling allowed the foam to expand and pack to a density twice that of the expected free-rise density.

The rise time for CRETE is approximately 8 min from the time of the pour. After the reaction was completed, the molds were cured at 66°C for a minimum of 4 h. After unmolding, right circular cylinders 28.7 mm in diameter and 50.8 mm long were cored from the foams. The cylindrical axis of these corings was always parallel to the rise direction of the foam. Care was taken to ensure that the cored samples did not contain any skin or any material from within 3 mm of the surface. The

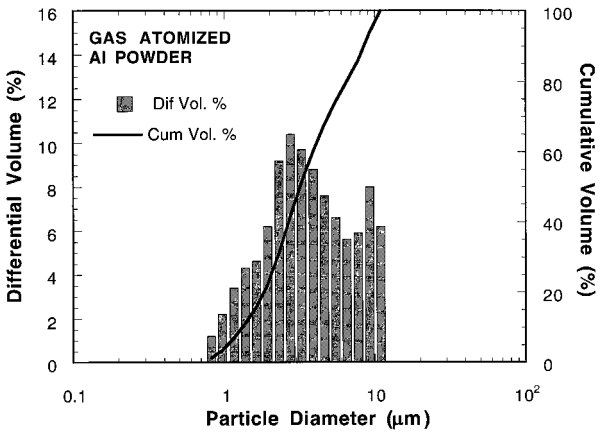

Figure 1 Size distribution for aluminum powder shown as differential and cumulative volume fractions versus particle diameter.

ends were machined to yield flat surfaces, and the cored sample densities were measured.

Formulation and Processing of Al-Filled CRETE Foam

Spherical, gas-atomized aluminum powder was purchased from Valimet Inc., Stockton, CA. A Microtrac® analysis was conducted by the powder supplier to verify the mean particle size and distribution. The results of this analysis are presented in Figure 1. From Figure 1, it can be seen that the median particle diameter is 3 μm and that more than 50 vol % of the powder consists of spheres between 2 and 4 μm in diameter. No powder particles were greater than 12 μm in diameter.

The as-received powder tended to agglomerate. To minimize this and to ensure uniform incorporation into the foam constituents, the powder was sieved using a Ro-Tap Sieve Shaker Model B from Tyler Inc., Mentor, OH. Testing sieves meeting ASTM E-11 specifications were used with a screen stacking sequence of 100, 200, and 325 mesh. Sieving was conducted in batches of four 100-mL scoops of powder for 1 h. Powder, sieved to $-100/+200$, was collected, and the process was repeated. This procedure resulted in powder that was more easily blended with the liquid constituents and in foams that were more uniform with respect to powder distribution within the cell walls and struts.

The Al-filled foam was formulated in an analogous manner to the unfilled foam detailed above. The exception was that the Al powder was added to the formulation after components 1–4 were hand-stirred. The fraction of filler (wt %) added to the CRETE matrix was defined as

$$\text{wt } \% = \frac{x}{x + \text{tot}} \tag{1}$$

where wt % is the weight percent of filler present in the composite, x is the weight of filler added, and tot is the total weight of all liquid constituents.

The formulation was once again stirred by hand. After the Al powder was completely wetted, the foam reaction was initiated with the addition of the isocyanate. The components were then mixed as before, poured into a mold, cured, and machined into cylindrical test specimens of the same dimensions, as described above.

Foam, which remained after the right circular samples were cored out, was cut into small strips and then snapped by hand to reveal a fracture surface for subsequent microscopy. The microstructure of the unfilled and Al-filled foams, as well as their fracture morphology, were examined using a JEOL 840 scanning electron microscope.

Mechanical Testing

All mechanical testing was conducted under ambient laboratory conditions on specimens ranging in foam density (ρ^*) (Terms or values annotated by an asterisk refer to parameters of the foam; other terms annotated by "$_{PU}$" refer to parameters related to the solid polymer.) from 0.05 to 0.91 g/cm^3. Since the density of solid polyurethane (ρ_{PU}) is 1.2 g/cm^3,[6] this range corresponds to normalized densities (ρ^*/ρ_{PU}) from 0.04 to 0.76 (for the unfilled foams). Mechanical properties in compression were evaluated on the right cylinders described above using a conventional Instron mechanical test frame. Tests were conducted in displacement control at a constant initial strain rate of 1.7×10^{-4} s^{-1}.

Moduli (E^*) were calculated as the slope of the linear portion of the compression loading curves. The modulus of CRETE measured in tension has been reported in a previous study.[5] Those results are included here for the sake of completeness. Macroscopic failure did not occur under quasi-static compressive loading for unfilled foam specimens and low loading fractions (less than 30 wt %) of the Al-filled foams. In these cases, tests were generally run to strains of approximately 0.3. Collapse stress, defined as the plateau in stress sub-

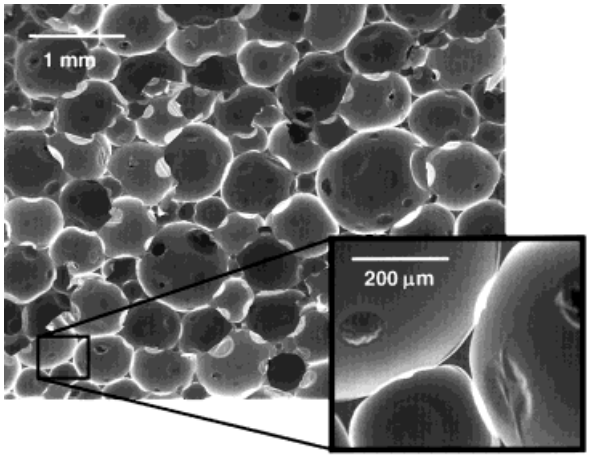

(a)

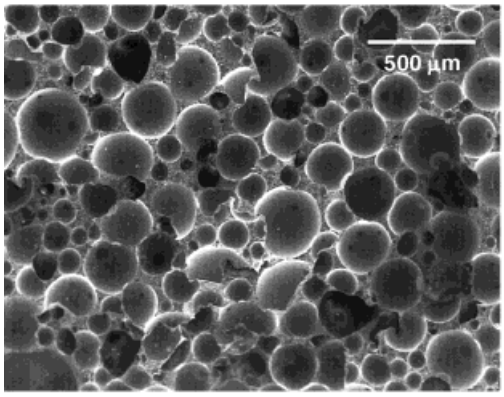

(b)

Figure 2 SEM micrograph of CRETE foam (a) $\rho^* = 0.12$ g/cm^3 (a typical polymer strut is shown in greater detail) and (b) $\rho^* = 0.36$ g/cm^3.

sequent to the initial linear loading region, was also measured as a function of specimen density.

RESULTS

Microscopy of Unfilled CRETE

Scanning electron microscopy was conducted on foam specimens to determine their structure and morphology. Figure 2(a) shows the typical microstructure of a foam specimen having a density of 0.12 g/cm^3. The cell microstructure is quite uniform and equiaxed with respect to the rise direction. Using a line intercept technique,[7] the average cell diameter is approximately 0.7 mm. The dimples on the cell walls represent the areas of contact between adjoining cells. These contact areas are continuous, thin polymer films, which, in fact, form the walls that enclose the cells. The intersection of several cells results in the formation of a cell strut, the principal structural member of the foam. A representative polymer strut is magnified in the insert in Figure 2(a) to illustrate this important feature. This high-magnification image reveals that the cell walls are very thin, only a few microns in thickness (thus, the majority of polymer resides in the struts). Increasing the CRETE density resulted in smaller cells, as illustrated in Figure 2(b) (note the difference in magnification). The structure is still uniform with an average cell diameter of 250 μm. At this higher density, the cell membranes are thicker on average than those seen in Figure 2(a).

Microscopy of Al-Filled CRETE

Scanning electron microscopy (SEM) analysis of the microstructure of the Al-filled foam revealed that, overall, the morphology of the cell structure was unaffected by the presence of the Al powder. That is, for any given foam density, the size and shape of the cells were the same for the loaded foams compared to the unloaded foams. At high magnifications, a uniform distribution of aluminum particles is found throughout the foam struts and cell walls of the foam. Figure 3(a)–(c) are scanning electron micrographs of the fracture surfaces of three Al-loaded specimens having a constant foam density of 0.28 g/cm^3 $\pm$ 0.01 and with increasing concentration of aluminum powder (5, 10, and 30 wt %, respectively). In each instance, a single strut is isolated to highlight the distribution of the aluminum powder.

The solid polymer struts are bounded by concave foam cells. With a concentration of only 5 wt %, it is seen in Figure 3(a) that the aluminum powder particles are widely separated. Increasing the fraction of aluminum to 10% yields a somewhat higher density of particles within the struts and cell walls, as shown in Figure 3(b). It is also apparent that a number of powder particles have pulled out of the polymer upon fracture leaving behind small dimples. Figure 3(c) shows the typical distribution of Al powder in a strut at 30 wt %. The faint features decorating the cell walls are Al particles that reside just below the free surfaces of the internal cell walls.

Compression Testing of Unfilled CRETE

A typical compression test is shown in Figure 4 for a foam having a density of 0.14 g/cm^3. After an

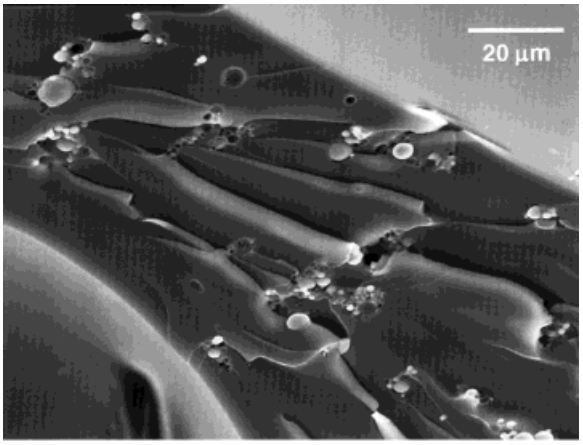

(a)

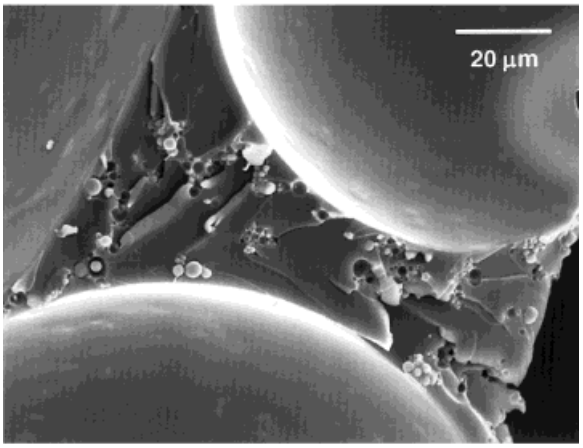

(b)

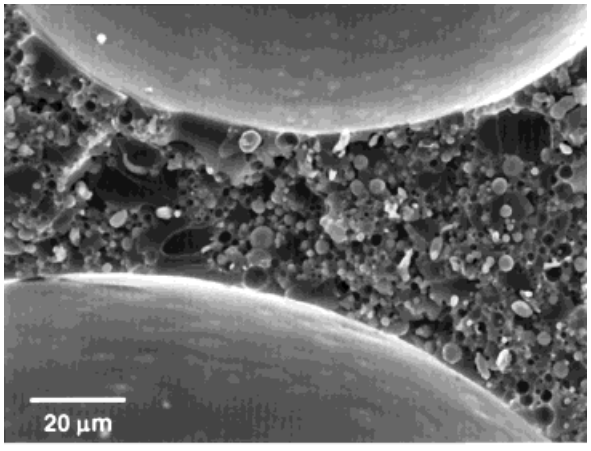

(c)

Figure 3 (a) Foam specimen (0.29 g/cm^3) containing 5 wt % Al. At this low loading, the aluminum powder particles occupy only a small volume fraction of the strut. (b) Foam specimen (0.28 g/cm^3) containing 10 wt % Al. Along with the higher concentration of powder particles, dimples are visible. These features arise from the debonding of the powder from the polymer strut. (c) Foam specimen (0.29 g/cm^3) containing 30 wt % Al. A high concentration of particles are seen randomly distributed within the strut and the cell walls.

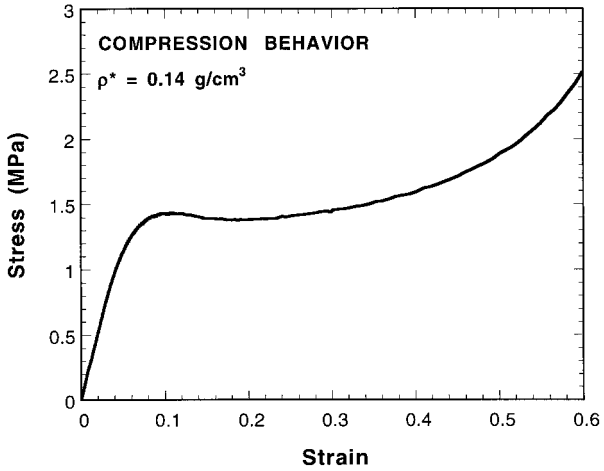

Figure 4 Compression test results for a foam, $\rho^* = 0.14$ g/cm^3. Yielding is abrupt and is followed by a sustained plateau region.

initial linear loading regime, the foam specimens show relatively abrupt yielding, followed by a sustained plateau region over which there is little increase in stress with increasing strain. The initial linear region defines the modulus of the foam. The broad plateau region results from the collapse or cell wall buckling of the foam[3] and, as previously indicated, is referred to as the collapse stress. At the lower densities, such as that shown in Figure 4, the stress after the plateau actually drops, giving rise to a yield pointlike behavior. At larger strains, subsequent to this plateau region, the stress increases as the foam begins to densify.

Moduli, derived from the compression tests, as a function of foam density are shown in Figure 5, along with tensile data from a previous study.[5] All of the data can be fit with a power-law expression with respect to density of the form, as follows:

$$E^* \propto (\rho^*)^n \tag{2}$$

where E^* is the modulus of the foam, ρ^* is the foam density, and n is the density exponent. Over the range of density shown in Figure 5, the data are well fit for a density exponent of $n = 1.7$. Figure 6 shows the same data plotted on a log–log

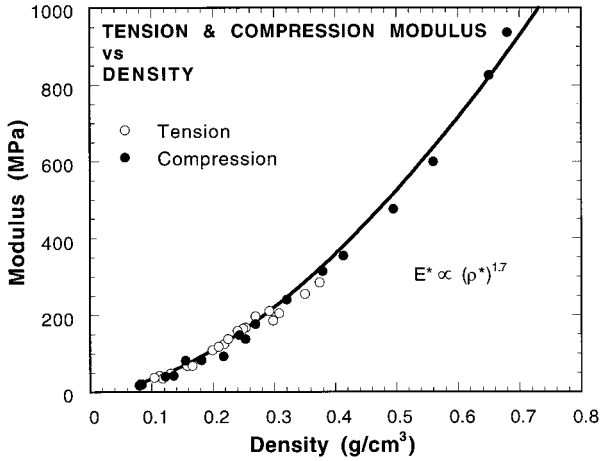

Figure 5 Density dependence of the modulus in tension and compression.

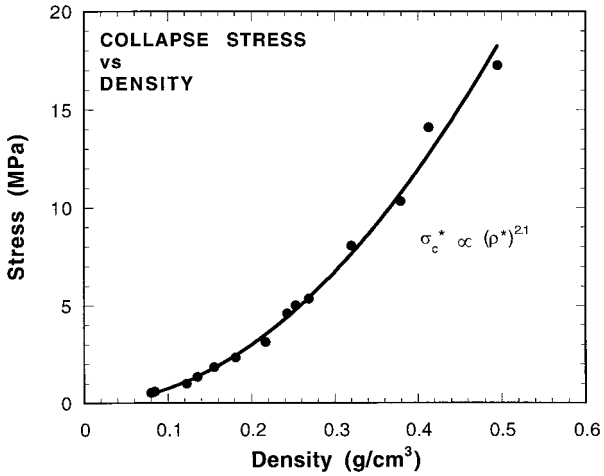

Figure 7 Power-law dependence of the collapse stress.

scale with the density normalized to that of the solid polymer, 1.2 g/cm^3. Thus, a specimen having a normalized density of 1 is equivalent to a fully dense monolithic polymer. In Figure 6, the data fall on a straight line with a slope of 1.7, confirming the power-law behavior. The intersection of the best-fit curve of the data and the ordinate for $\rho^*/\rho_{PU} = 1$ can be taken to be the modulus of the solid polymer. By doing so, we arrive at a value of the solid modulus of 2.5 GPa. This is within the range of reported values for E_{PU} of 1.6 to 2.7 GPa.[6,8]

The collapse stress σ_c^* for the foam specimens as function of density is shown in Figure 7. This is an important parameter in the design of cushions for shock or impact mitigation because it represents the onset of the mechanical instability of the foam microstructure.[3] It, too, exhibits a power-law dependence with respect to foam density, although the density exponent, 2.1, is somewhat higher than that exhibited by the modulus. When plotted on logarithmic axes, the data shown in Figure 7 would fall along a straight line similar to the data shown in Figure 6 (although with a scope equal to 2.1).

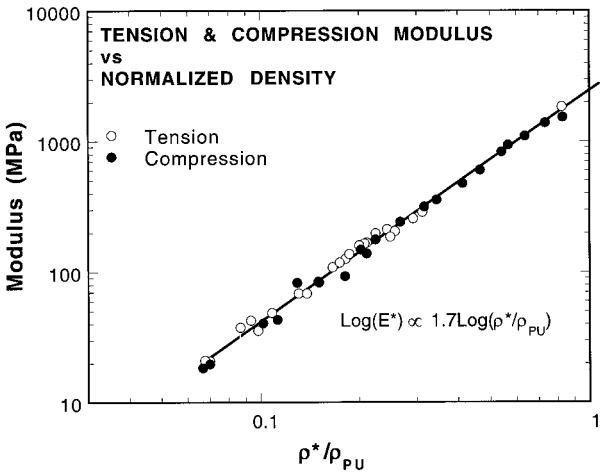

Figure 6 Log–log plot showing power-law behavior between modulus and normalized density. The intersection of the best fit curve and the ordinate for $\rho^*/\rho_{PU} = 1$ is used as the modulus of the solid polymer hereafter.

Compression Testing of Al-Filled CRETE

In order to directly observe the influence of the aluminum additive on the mechanical properties of the unfilled foam, a common reference state must be established. We choose to compare behavior between the unfilled and Al-filled foam on the basis of polymer density. For the case of the filled foams, the polymer density is calculated from the measured aggregate density of the filled specimen and the weight fraction of the aluminum added. For example, for a specimen having an aggregate density of 0.68 g/cm^3 that contains 10 wt % Al, the calculated polymer density is 0.63 g/cm^3.

With this basis of comparison, the influence of the Al powder mechanical properties is readily seen in Figure 8. This figure shows a series of compression stress–strain curves for loaded specimens having a constant polymer density of 0.28 g/cm^3. It is clear from Figure 8 that progressively increasing the fraction of powder in a foam that has a constant polymer density increases both the

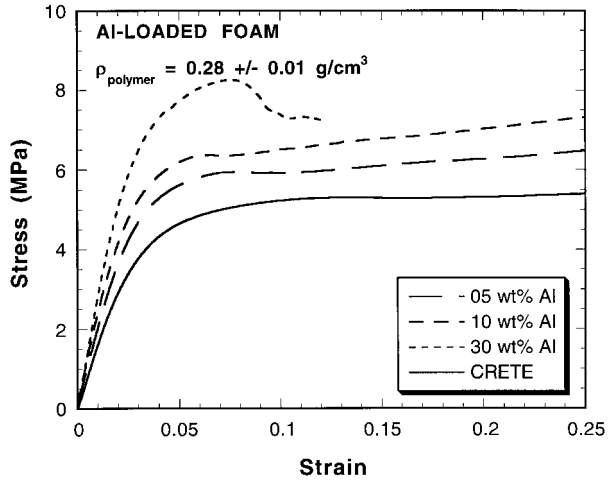

Figure 8 Comparison of the compressive behavior of the Al-filled CRETE to the unfilled CRETE foams.

elastic modulus and the strength of the foam. In all cases, the Al-loaded specimens have moduli that are greater than that of the unloaded specimens. The magnitude of the increase is dependent upon the amount of filler added. Additions of 5 and 10 wt % have a small effect on modulus. In the examples shown in Figure 8, 5 and 10 wt % additions of powder are found to increase the modulus from 175 to 190 and 206 MPa. These represent 8 and 17% increases, respectively. The modulus of the foam specimen containing 30 wt % filler exhibits a modulus of approximately 280 MPa, a 60% increase.

The aluminum filler also affects the collapse stress of the foam. The collapse stress of the unfilled foam is 5.3 MPa and 5 and 10 wt % additions of aluminum increase σ_c^* to 6.0 and 6.4 MPa (13 and 21% increases, respectively). It is also seen from Figure 8 that at 30 wt % Al, the strength of the foam is about 25% greater than that of the unloaded foam, 8.3 MPa.

However, the sample loaded to 30 wt % Al fails at a strain of 0.13 (for the other specimens, the tests were terminated at about strains of about 0.25). Unlike the unloaded foam specimen or specimens with low loading fractions, this specimen showed evidence of cracking with increasing strain. Such cracking at low strains is uncharacteristic of polyurethane foams of this density and stems from the fact that some of Al powder is either poorly bonded to the polymer matrix initially or dewets during deformation. Thus, while the powder may act to strengthen the foam, some of the individual particles act as preexisting defect sites, allowing for easier crack initiation and propagation. At low concentrations, this effect is small, and ductility is largely unaffected. This same dewetting phenomena accounts for the dramatic yield point behavior shown in Figure 8 that was exhibited by the specimen containing the highest loading fraction of filler. As the filler dewets during deformation and the adhesion between it and the matrix is compromised, the composite modulus is reduced. When tested at a fixed displacement rate, the decreased modulus results in a drop in the observed load.

The influence of the rigid filler phase on the modulus of the foam over a wide range of polymer density is shown in Figure 9. This figure compares the original modulus data for the unfilled foam shown in Figure 5 to specimens containing controlled additions of the aluminum powder filler. The abscissa is the calculated polymer density, as was described at the beginning of this section. The solid line represents a best fit through the unfilled foam data previously presented in Figure 5. The corresponding data points are omitted for clarity. The measured moduli for the specimens containing 5, 10, 30, and 50 wt % are also shown in this figure. It is seen that the power-law dependence, $n = 1.7$, denoted by the traces through each set of data, still describes the density dependence of the modulus for each loading fraction of aluminum.

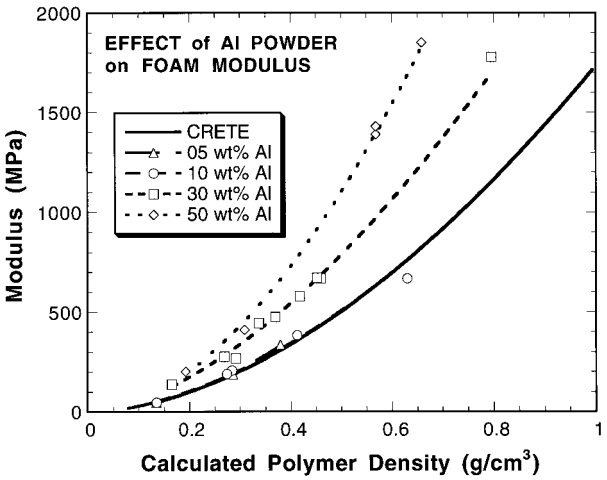

Figure 9 Influence of Al powder additions on the CRETE modulus. Modulus increases with loading percent and still exhibits the 1.7 power law dependence on CRETE density. The solid line represents the best fit through the data in Figure 5. The abscissa is the calculated density of each foam specimen, regardless of the loading fraction of aluminum, as defined by eq. (1).

It is clear from Figure 9 that aluminum loadings of 5 and 10 wt % have only a small effect on the modulus of the foam. It is only at the higher loading fractions of 30 and 50 wt % (volume fractions of about 0.15 and 0.30, respectively) that a significant increase in modulus is observed. For example, at relatively low polymer densities ($\rho = 0.3$ g/cm^3), the modulus of the loaded foams can be more than doubled by the addition of 50 wt % Al powder.

That the modulus of the foam is found to increase at powder concentrations greater than 30 wt % is not unexpected. The effect may be attributed to the formation of a nearly continuous network of aluminum powder at these higher loading fractions. For a random dispersion of spherical particles, it has been shown that a continuous network is formed at the critical volume fraction 30%.[4] This volume fraction corresponds to an aluminum weight concentration of approximately 50 wt %, about where the most significant increase in foam modulus was observed.

DISCUSSION

Relationship Between the Modulus and Strength of Foams and Their Structure

The dependence of both the modulus and the elastic collapse stress of a cellular foam can be understood in terms of the mechanical properties of the polymer material from which the cell struts (and in the present case, the cell walls) are made and the deformation mechanics of the cellular structure itself. Elastic moduli are related principally to the bending stiffness of the members comprising the cellular structure, while the elastic collapse is caused by the elastic buckling of these same members.

For the discussion presented below, the important cell strut/wall properties are the solid polymer density ρ_s and its modulus E_S. The important structural features for the analysis of the modulus and the collapse stress are the normalized density of the foam ρ^*/ρ_s (as before, ρ^* is the density of the foam) and whether or not the cells are open or closed. In this regard, a parameter, ϕ, is defined as the fraction of material in the cell struts. For an open-cell foam, $\phi = 1$, while for a closed-cell foam, where some of the polymer is in the cell walls, it is less than 1.

Modulus

Gibson and Ashby[3,9] have put forth a simple model that has been shown to accurately describe the density dependence of the modulus for CRETE (and other) foams. In their model, a foam is described as an array of cubic cells consisting of struts (that define the cell edges) and walls (that enclose the cells in a closed-cell foam). These cells are then staggered so that corners of one cell rest upon the midpoint of adjacent cells. Such a structure does not correspond to the actual geometric characteristics of a real foam, nor can it be reproduced to fill space. It does, however, capture the critical physical processes that govern the deformation processes of a cellular structure. Described in this fashion, the modulus of such a structure is related to the elastic deflection of the struts that are oriented normal to an applied far field load.

For an open-cell foam, where all of the polymer resides in the cell struts, Gibson and Ashby arrive at the following simple expression for the density dependence of the modulus of a foam:

$$\frac{E^*}{E_s} \approx \left(\frac{\rho^*}{\rho_s}\right)^2 \tag{3}$$

Equation (3) predicts that a parabolic relationship should exist between the modulus of the foam and its density. The data in Figure 5 suggest, however, that the power-law exponent is less than 2. This discrepancy can be found in the fact that the foam has a closed-cell structure rather than an open-cell structure. As such, some fraction of the polymer resides in the cell walls or faces rather than solely in the struts.

If the fraction of polymer contained in the cell struts is ϕ, then the fraction contained in the cell walls is $(1 - \phi)$. The modulus of a closed-cell foam (ignoring internal gas pressure) results then from two contributions. The first component is strut bending, as for open-cell foams. The second component arises from the stretching of the cell wall faces.[10–12] Gibson and Ashby[3,9] derive the modulus of a closed-cell foam, which accounts for these two components, as follows:

$$\frac{E^*}{E_s} \approx \phi^2\left(\frac{\rho^*}{\rho_s}\right)^2 + (1 - \phi)\left(\frac{\rho^*}{\rho_s}\right) \tag{4}$$

The first term on the right describes the contribution of the cell struts to the modulus, while the second term accounts for the stretching of the cell walls. Equation (4) predicts a pseudo power-law relationship with respect to density, in which the density exponent increases continuously from 1 to

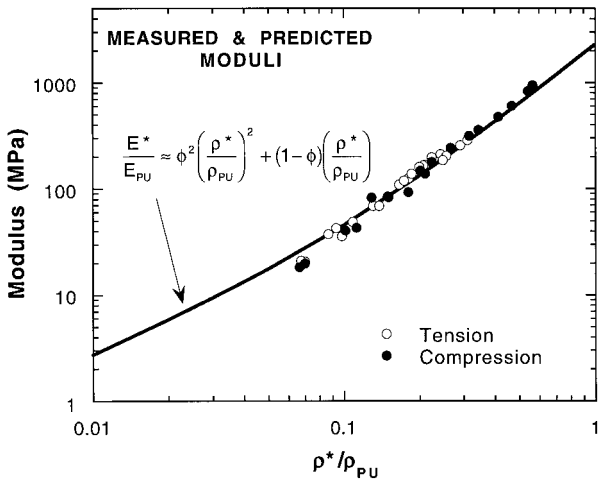

Figure 10 Comparison of modulus measurements to eq. (4). Note that density is normalized to the density of the solid polymer. The partitioning factor is held constant at $\phi = 0.9$.

2 with increasing ρ^*/ρ_s. Over the density range of the measurements reported here, eq. (4) describes the functional dependence of modulus on density with an exponent close to that which best fits the data shown in Figure 5.

The data shown in Figure 5 can be quantitatively compared to eq. (4) using known values for ρ_s and E_s and ϕ. For the density of solid polyurethane, we use a value of $\rho_s = \rho_{PU} = 1.2$ g/cm^3.[6] The value for the modulus of solid polyurethane is less well established and varies considerably, depending on the precise formulation, processing conditions, and product form. Since the value for the modulus of solid polyurethane is less certain, we use the value obtained from Figure 6, $E_s = E_{PU} = 2.5$ GPa. For ϕ, we use a value of 0.9. (Note: We have not independently measured ϕ for this foam system; the value used, $\phi = 0.9$, is typical for polyurethane foams.[13]) Using these values, the comparison between eq. (4) and the data in Figure 5 is shown in Figure 10. The figure shows that the model represents the data well over the range of densities examined experimentally.

Collapse Stress

The dependence of the plateau stress on foam density has also been address by Gibson and Ashby.[3,9] As the applied load increases, cell struts that are parallel to the load become unstable. This instability is termed "lateral buckling," and the applied load necessary to cause it is called the "Euler buckling load." The derivation of the Euler buckling load is a well-known problem in mechanics[14] and, when incorporated into the geometric model of Gibson and Ashby, can be used to predict the mechanical collapse of a foam as

$$\frac{\sigma_c^*}{E_s} = C \times \left(\frac{\rho^*}{\rho_s}\right)^2 \left(1 + \left(\frac{\rho^*}{\rho_s}\right)^{1/2}\right)^2 \qquad (5)$$

where the constant C contains all of the physical and geometric factors relevant to the foam polymer and structure. In principle, the constant C can be explicitly calculated. However, it is more expedient to fit the measured collapse stress data shown in Figure 7 to eq. (5), using C as a fitting parameter. As shown in Figure 11, eq. (5) best fits the data for C = 0.02. As for the modulus prediction, the prediction derived by Gibson and Ashby for the collapse stress accurately reflects the density dependence of the foam over the range of densities measured.

Prediction of Al-Filled Foam Properties

The strut of a particulate-filled polyurethane foam is essentially a polymer–matrix composite consisting of two or more separate constituents, a continuous matrix phase and a discontinuous filler phase. The change in properties of a foam containing a rigid phase (from that of an unloaded foam) should track with the effect of the additive on the properties of the monolithic polymer. Thus, it should be possible, therefore, to predict the

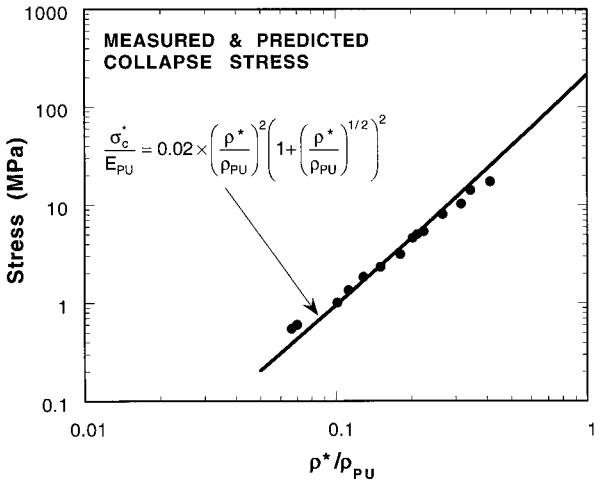

Figure 11 Comparison of collapse stress measurements to eq. (5) versus normalized density.

behavior of the Al-filled foam by understanding the effect of the filler phase on the host matrix.

Much work has been done in regards to characterizing the effect of filler phases on the properties of resin matrix composites. Palumbo et al. have studied the mechanical behavior of a composite consisting of a fully dense epoxy matrix and hollow glass microspheres (GMB).[15] Results of this work revealed that the modulus of the composite decreased with increasing loading fraction of the GMB, which has a lower modulus than the host epoxy matrix. In another study, Domeier et al. found much the same effect in a similar epoxy/GMB composite system.[16] In contrast, Monette et al. observed an increase in Young's modulus when silica beads were dispersed throughout an epoxy matrix.[17] The experimental data revealed an increasing elastic modulus as the volume fraction of filler was increased. Similar findings were reported for an epoxy/alumina system.[16] In both instances, the modulus of the additives were greater than that of the matrix yielding composite structures of overall greater stiffness.

Beyond these experimental investigations, there have been many other studies[18,19] devoted to modeling the elastic properties of composites. The two most widely used methods for predicting the mechanical properties of particulate-reinforced composites are those developed by Hashin and Shtrikman[20] and Kerner.[21]

In the latter reference, a composite is considered to be a distribution of spherical particles suspended in a homogeneous matrix. The analysis assumes that there exists an average state of stress and strain within each particle when subjected to a hydrostatic stress. Kerner then formulated expressions for the bulk and shear moduli of a composite in terms of the bulk and shear moduli of both the matrix solid and filler phases, their respective volume fractions, and Poisson's ratio of the matrix.

The resulting Kerner equations are quite complicated and can be difficult to apply. Halpin and Tsai[22–24] showed that by grouping terms that pertain to the Poisson effect and particle geometry and, also, separating terms, which depend on the elastic properties of the constituents, the Kerner equations can be generalized to the following form:

$$\frac{M_c}{M_m} = \frac{1 + AB\theta_f}{1 - B\theta_f} \tag{6}$$

where M_c and M_m are any composite and matrix moduli and matrix and θ_f is the volume fraction of the filler phase.

$$A = \frac{7 - 5\nu_m}{8 - 10\nu_m} \tag{7}$$

where ν_m is Poisson ratio of the matrix and

$$B = \frac{(M_f/M_m) - 1}{(M_f/M_m) + A} \tag{8}$$

where M_f is the modulus of the filler.

Specifically, for the Young's modulus of a particle-filled composite,

$$E_c = E_m\left[\frac{1 + AB\theta_f}{1 - B\theta_f}\right] \tag{9}$$

where E_c is the composite modulus and E_m is that of the host matrix.

The measured moduli of traditional reinforced polymer composites have been compared favorably with predictions based on eq. (9).[15,16]

Modulus for Al-Loaded CRETE

It has been shown in Figures 2 and 3 that the Al powder is uniformly incorporated into the cell strut and cell wall elements of the foam. Therefore, these elements of the foam structure can be modeled as a composite with a matrix phase of solid polyurethane and a reinforcing phase of Al powder. As such, it should be possible to use the Halpin–Tsai equation in conjunction with the Gibson and Ashby model for the modulus of a closed-cell foam to predict the modulus of the Al-filled foam. In this case, the matrix modulus E_m is the modulus of solid polyurethane E_{PU}. E_c then represents the modulus of the filler-loaded strut (i.e., the composite) and is substituted for E_s (the modulus of the foam strut material). In an analogous fashion, ρ_s is now the density of the PU–Al powder composite at each loading fraction of aluminum and is termed ρ_{comp}. Finally, ρ^* is replaced by the total aggregate density of a specimen, ρ_{sample}. These new terms for the modulus and density of the PU–Al powder composite and specimens can be substituted into eq. (4).

The final governing expression for the modulus of the powder-loaded PU foam is given as

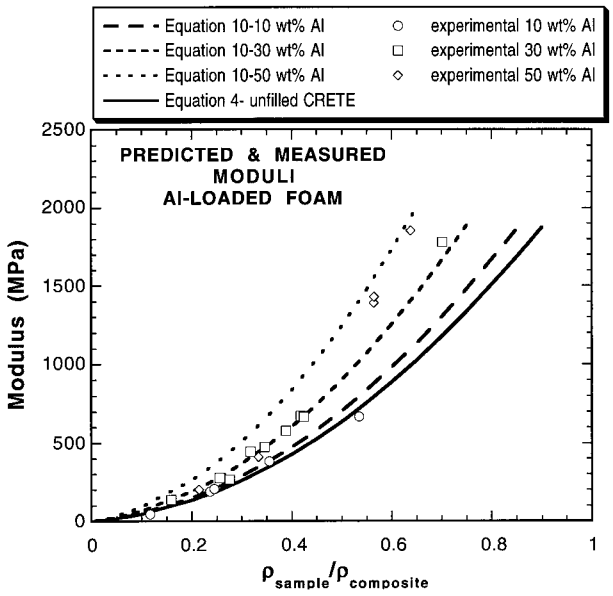

Figure 12 Combined Halpin–Tsai and Gibson and Ashby predictions for the modulus of a powder-filled foam.

$$E^* \approx E_{\mathrm{PU}}\left[\frac{1 + AB\theta_f}{1 - B\theta_f}\right]\left[\phi^2\left(\frac{\rho_{\mathrm{sample}}}{\rho_{\mathrm{comp}}}\right)^2 + (1 - \phi)\left(\frac{\rho_{\mathrm{sample}}}{\rho_{\mathrm{comp}}}\right)\right] \quad (10)$$

Substituting appropriate values into eqs. (7) and (8), the parameters A and B can be calculated. As before, the modulus of solid polyurethane is taken to be 2.5 GPa. The modulus of aluminum is 68.9 GPa.[25] Poisson's ratio for polyurethane is taken as 0.35[26] and the partitioning factor ϕ was once again held constant at 0.9.

Figure 12 compares the experimentally measured moduli to the predicted moduli for Al-loaded foam. The data for the aluminum filled foam are the same as those previously presented in Figure 9. The solid line corresponding to the unfilled foam represents the modulus predicted by eq. (4). The data points have been omitted for clarity. The additional traces show the predicted density dependence of the modulus from eq. (10) for each loading fraction of aluminum. Note that both the data and the prediction for the 5 wt % aluminum samples are not shown since both show little difference from the unfilled foam. It is seen that the final governing equation captures the effect of the aluminum powder on the foam modulus well. The combined Halpin–Tsai form of the Kerner equation and Gibson and Ashby model accurately predicts the density dependence of the modulus as well as the increase in modulus for each loading fraction. It accurately predicts that there is little effect on foam modulus for low (5 and 10 wt %) loading fractions of aluminum. Equation (10) also predicts the significant increase in foam modulus for 30 and 50 wt %.

Collapse Stress for Al-Loaded CRETE

Equation (5) predicts that for foams of constant density, the collapse stress should vary as a linear function of the modulus of the strut and cell wall material. By combining eqs. (5) and (9), the predicted collapse stress is

$$\sigma_c^* = 0.02 \times E_{\mathrm{PU}}\left[\frac{1 + AB\theta_f}{1 - B\theta_f}\right]\left(\frac{\rho_{\mathrm{sample}}}{\rho_{\mathrm{comp}}}\right)^2 \times \left(1 + \left(\frac{\rho_{\mathrm{sample}}}{\rho_{\mathrm{comp}}}\right)^{1/2}\right)^2 \quad (11)$$

should track with the collapse stress values shown in Figure 8. Such a comparison is shown in Figure 13, where the data points represent the measured collapse stress values from Figure 8, and the trace represents the expected collapse stress based on eq. (11). The trace representing the prediction is always somewhat higher than the actually measured collapse stress. This is to be expected as the Halpin–Tsai model assumes complete adhesion between the filler phase and the matrix. Since both the microscopy in Figure 3

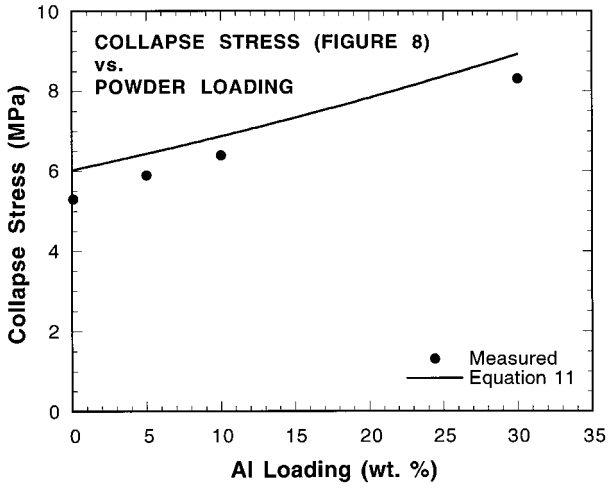

Figure 13 Comparison of combined Halpin–Tsai and Gibson and Ashby predictions for the collapse stress of a powder-loaded foam.

and the mechanical properties shown in Figure 8 suggest less than complete adhesion, it is not surprising that the full strengthening potential of the filler is not realized. Notwithstanding this, the agreement between the data and the collapse stresses predicted by eq. (11) is quite good. As with the modulus, this generally good agreement suggests that the behavior of the powder loaded foam can be modeled as that of a cellular composite.

CONCLUSIONS

Scanning electron microscopy revealed that the structure of the CRETE foam formulation was uniform with respect to cell size and shape. Addition of aluminum powder did not alter the uniformity of the foam structure. A random nonagglomerated distribution of aluminum powder throughout the cell struts and walls was evident.

The modulus of the unfilled foam was increased with the addition of aluminum powder. The experimental data tended to group by loading fraction with 5 and 10 wt % additions showing only minor increases in modulus. However, as the weight fraction of filler was increased to 30 and 50 wt %, the foam modulus increased significantly. A 2 to 3-fold increase in modulus can be realized at the highest loading fractions examined in this study. The density dependence of the modulus was unaffected by the additions of the filler phase. Over the range of densities examined the strength of the filled foam was greater than that of the unfilled foam for all loading fractions of aluminum. However, high loading fractions produced a yield point behavior and caused the foam to be susceptible to cracking. This was the result of the poor adhesion between the aluminum powder and the polyurethane matrix.

For the unfilled foam, the good agreement between the measured modulus and the collapse stress with the predictions of eqs. (4) and (5) suggests that a model available in the literature, based on a simple, idealized cell geometry, can be useful in these mechanical and physical properties of foams. By considering the strut of the filled foam to be a composite consisting of a rigid phase within a polyurethane matrix, the increase in the modulus and strength of the Al-loaded foam could be understood. A well-known expression that describes the effect of rigid, spherical additives on the modulus of monolithic composites was incorporated into the Gibson and Ashby foam model. By combining these two models, expressions that accounted for both the composite nature of the solid and the overall foam structure were created. These expressions were shown to reasonably predict the effect of a rigid filler phase on both the modulus and strength of the filled foam.

The authors thank Mike Tootle for his help in sample preparation and testing and Nancy Yang and Eric Kleinschmidt for microscopy support. This work supported under U.S. Department of Energy contract #DE-AC04-94AL85000.

REFERENCES

1. Klempner, D.; Frisch, K. C. Handbook of Polymer Foams and Foam Technology; Oxford University Press: New York, 1991; pp. 47–94.
2. Hilyard, N. C.; Cunningham, A. Low Density Cellular Plastics, Physical Basis of Behaviour; Chapman and Hall: London, UK, 1994; p. 104.
3. Gibson, L. J.; Ashby, M. F. Cellular Solids, Structure, and Properties; Pergamon Press: New York, 1988.
4. Bhattachara, S. K. Metal-Filled Polymers: Properties and Applications; Marcel Dekker: New York, 1986; pp. 5–15, 172.
5. Goods, S. H.; Neuschwanger, C. L.; Henderson, C.; Skala, D. M. J Appl Polym Sci 1998, 68, 1045.
6. Roff, W. F.; Scott, J. R. Fibres, Films, Plastics and Rubbers—A Handbook of Common Polymers, Butterworths: London, UK, 1971; p. 445.
7. Underwood, E. E. Quantitative Stereology; Addison-Wesley Publishing Co.: Reading, MA, 1970.
8. Plastics Digest, Vol. 2; D.A.T.A.: Englewood, CO, 1994, pp. 1301–1304.
9. Gibson, L. J.; Ashby, M. F. Proc R Soc London 1982, A382, 43.
10. Patel, M. R.; Finnie, I. J Mater 1970, 5, 909.
11. Green, D. J. J Am Ceram Soc 1985, 68, 403.
12. Christensen, R. M. J Mech Phys Solids 1968, 34, 563.
13. Reitz, D. W.; Schuetz, M. A.; Glicksman, L. R. J Cell Plast 1984, 20, 104.
14. Timeshenko, S.; Young, D. H. Elements of Strength of Materials, 4th ed.; D. van Nostrand & Co. Inc.: New York, 1962; pp. 212, 342.
15. Palumbo, M.; Donzella, G.; Tempesti, E.; Ferruti, P. J Appl Polym Sci 1996, 60, 47–53.
16. Domeier, L.; Skala, D. M.; Goods, S. H.; Neuschwanger, C. L.; Tootle, M. L.; Lu, W. SAND98-8204, Sandia National Laboratories, Livermore, CA, 1998.
17. Monette, L.; Anderson, M. P.; Wagner, H. D.; Mueller, R. R. J Appl Phys 1994, 75, 1442.

18. Paul, B. AIME Trans 1960, 218, 36.
19. Bohme, R. D. J Appl Polym Sci 1968, 12, 1097.
20. Hashin, Z.; Shtrikman, S. J Mech Phys Solids 1963, 11, 127.
21. Kerner, E. H. Proc Phys Soc London 1956, B69, 808.
22. Halpin, J. C. J Comp Mater 1969, 3, 732.
23. Halpin, J. C. Primer on Composite Materials Analysis, 2nd ed.; Technomic Publishing: Lancaster, PA, 1992; p. 161.
24. Tsai, S. W. US Government Report AD 834851, 1968.
25. Smithells, C. J.; Brandes, E. A. Metals Reference Book, 5th ed.; Butterworths: Woburn, MA; 1976.
26. Birley, A. W.; Haworth, B.; Batchelor, J. Physics of Plastics—Processing, Properties and Materials Engineering, Oxford University Press: New York, 1991; p. 255.